

Peculiar velocities of galaxies in the Leo Spur¹

Igor D. Karachentsev

Special Astrophysical Observatory, the Russian Academy of Sciences, Nizhnij Arkhyz,
Karachai-Cherkessian Republic, Russia 369167

ikar@sao.ru

R. Brent Tully

Institute for Astronomy, University of Hawaii, 2680 Woodlawn Drive, Honolulu, HI 96822,
USA

Lidia N. Makarova

Special Astrophysical Observatory, the Russian Academy of Sciences, Nizhnij Arkhyz,
Karachai-Cherkessian Republic, Russia 369167

Dmitry I. Makarov

Special Astrophysical Observatory, the Russian Academy of Sciences, Nizhnij Arkhyz,
Karachai-Cherkessian Republic, Russia 369167

Luca Rizzi

W. M. Keck Observatory, 65-1120 Mamalahoa Hwy, Kamuela, HI 9 6743, USA

Received _____; accepted _____

ABSTRACT

Hubble Space Telescope Advanced Camera for Surveys has been used to determine accurate distances for the spiral galaxy NGC 2683 and 12 other galaxies in a zone of the "local velocity anomaly" from measurements of the luminosities of the brightest red giant branch stars. These galaxies lie in the Leo Spur, the nearest filament beyond our home Local Sheet. The new, accurate distance measurements confirm that galaxies along the Leo Spur are more distant than expected from uniform cosmic expansion, hence have large peculiar velocities toward us. The motions are generally explained by a previously published model that posits that the Local Sheet is descending at 259 km/s toward the south supergalactic pole due to expansion of the Local Void and being attracted at 185 km/s toward the Virgo Cluster. With the standard Λ CDM cosmology an empty void expands at 16 km/s/Mpc so a motion of 259 km/s requires the Local Void to be impressively large and empty. Small residuals from the published model can be attributed to an upward push toward the north supergalactic pole by expansion of the Gemini-Leo Void below the Leo Spur. The Leo Spur is sparsely populated but among its constituents there are two associations that contain only dwarf galaxies.

Subject headings: galaxies: distances and redshifts — galaxies: dwarf — large-scale structure of universe — dark matter

1. Introduction

The anisotropic nature of gravitational collapse leads to formation of the cosmic large-scale structure, whose basic elements are walls (“pancakes”), filaments, and clusters (“nodes”) on their intersection (Zeldovich 1970, Peebles 1980, Shandarin et al. 2012). According to the results of N-body simulations, about 77% of the volume fraction of the Universe is occupied by cosmic depressions (voids), while about 50% of the total mass is concentrated within filaments (Cautun et al. 2014).

Computer simulations predict that filaments and walls can move relative to each other with velocities of several hundred km/s. Bulk motions of the same order are expected along the filaments towards rich clusters (Shandarin & Klypin 1984, Shandarin & Zeldovich 1989, van Haarlem & van de Weygaert 1993). Observational confirmation of these predictions are extremely scarce because they require precise distances to many galaxies measured independently from their radial velocities.

To date, we know that the nearest and the most completely studied flat configuration of a dozen nearby groups, called the “Local Sheet”, is a rather cold structure with a characteristic dispersion of peculiar (non-Hubble) velocities $\sigma_v \sim 40$ km/s (Karachentsev et al. 2003, Tully et al. 2008). Recently, Brinckmann et al. (2014) found similar sheets with $\sigma_v \sim 100$ km/s near the rich Coma Cluster.

According to Tully et al. (2008, 2013), the Local Sheet as a whole is moving toward a nearby cloud of galaxies called the Leo Spur in the “Nearby Galaxies Atlas” (Tully &

¹Based on observations made with the NASA/ESO Hubble Space Telescope, obtained at the Space Telescope Science Institute, witch operated by the Association of Universities for Research in Astronomy, Inc., under NASA contract NAS 5–26555. These observations are associated with program SNAP 13442.

Fisher 1987) with a velocity of ~ 320 km/s. The basic components of this bulk motion of the Local Sheet are its infall towards the nearby Virgo Cluster, as well as motion away from the Local Void, with velocities ~ 190 km/s and ~ 260 km/s, respectively. Addition of the vectors leads to appearance on the sky of the zone of a "Local Velocity Anomaly" in Gemini-Cancer-Lynx constellations, a subject of discussion since the 1980's (Faber & Burstein 1988, Tully 1988a).

In supergalactic coordinates, the galaxies in the Local Sheet lie in the equatorial band, $SGZ = 0$, stretching toward the Virgo Cluster. The Local Void lies toward the positive pole. The Leo Spur lies in a plane roughly parallel to the Local Sheet toward the negative pole. Below the Leo Spur is the "Gemini-Leo" Void, No. 27 in the list of nearby volumes completely devoid of galaxies (Elyiv et al. 2013). The void center is near $RA = 7^h8$, $Dec. = +24^\circ$ at a distance of 18.4 Mpc and its radius is 7.5 Mpc, or 24° . The Local Sheet and the Leo Spur are moving toward each other, squeezed between two inflating voids. Accurate measurements of the relative motions provide insight into the importance of the juxtaposed voids.

The Leo Spur contains several dozen galaxies with radial velocities less than 500 km/s, but accurate distances have only recently become available for a subset. The program "The Geometry and Kinematics of the Local Volume" with Hubble Space Telescope, GO 12546 & 13442 (PI: R.B.Tully) supplemented by program GO 12658 (PI: J. Cannon), has gone a long way toward augmenting the galaxy census in this area by facilitating distance determinations with the tip of the red giant branch (TRGB) method. Below, we present a summary of observational data on distances and peculiar velocities of galaxies in the sky region $RA = [5^h15^m - 11^h30^m]$, $Dec = [-8^\circ - +56^\circ]$, with velocities in the Local Group rest frame below $V_{LG} = 500$ km/s. The compilation includes new accurate distance measurements for the luminous spiral galaxy NGC 2683 and for 12 dwarf galaxies.

2. ACS HST observations and data processing

We have observed 10 galaxies with Advanced Camera for Surveys (ACS) during HST Cycle 21 (proposal 13442) that are relevant to the present discussion. Between October 25, 2013 and April 21, 2014 we obtained 1000s F606W and 1000s F814W images of each galaxy using ACS/WFC with exposures split to eliminate cosmic ray contamination. In addition we have reduced and analyzed images obtained for three galaxies in the relevant region observed during cycle 19 with proposal 12658 (PI: J. Cannon). Additional material from HST program 12546 and earlier was discussed by Jacobs et al. (2009) and is included in the *Cosmicflows-2* data release (Tully et al. 2013) and made available at the Extragalactic Distance Database.²

The new images were obtained from the STScI archive, as processed according to the standard ACS pipeline. The stellar photometry was performed using the ACS module of DOLPHOT (<http://americano.dolphinsim.com/dolphot>), the successor to HSTPHOT (Dolphin 2000), using the recommended recipe and parameters. In brief, the process involves the following steps. First, pixels that are flagged as bad or saturated in the data quality images were marked in the data images. Second, pixel area maps were applied to restore the correct count rates. Finally, the photometry was run. In order to be reported, a star had to be recovered with S/N of at least four in both filters, $|sharp| \leq 0.3$, be unsaturated and relatively clean of bad pixels (such that the DOLPHOT error flag is zero) in both filters. These restrictions reject non-stellar and blended objects. At the high Galactic latitudes of the targets, foreground stars from the Milky Way are insignificant contaminants. All the observed galaxies are resolved into individual stars including those on the red giant branch (RGB), allowing a distance to be measured with the tip of the red giant branch (TRGB) method.

²<http://edd.ifa.hawaii.edu/catalog/CMDs/TRGB>

The TRGB is determined by a maximum likelihood analysis monitored by recovery of artificial stars (TRGBtool software, Makarov et al. 2006). Artificial stars with a wide range of known magnitudes and colors are imposed over the frame in numbers relative to the density of the real stars and recovered (or not) with the standard analysis procedures to determine both photometric errors and completeness in the crowded field environments. The maximum likelihood procedure evaluates the luminosity function of stars with colors consistent with the red giant branch after compensating for completeness and assesses power law fits to the distributions above and below a break identified with the TRGB. The slope of the power law faintward of the TRGB break is expected to be approximately 0.3 on a magnitude scale after correction for completeness. If the RGB is sufficiently observed to well below the tip then the slope can be a free parameter within a restricted range but in the current cases, with distances approaching the effective observational limits, the slope of the luminosity function fit below the TRGB is set to the expected value of 0.3. Galactic extinction is taken from Schlafly & Finkbeiner (2011).

The greatest potential for serious error with a TRGB measurement arises with confusion between the intermediate age asymptotic giant branch (AGB) and the RGB. Stars on the AGB, that are burning both helium and hydrogen in shells, closely parallel and overlap the RGB on a CMD but rise as much as a magnitude brighter. Their peak brightness, dependent on age and metallicity, can be misinterpreted as the TRGB. AGB stars have intermediate ages of 1-10 Gyr although they are only in sufficient quantity to be confusing at the lower end of that age range (Jacobs et al. 2011). A general strategy that we employ is clipping of the area of the HST image to avoid regions of young and intermediate age stars and associated obscuration (as well as regions beyond the target dominated by background and foreground contaminants) in order to maximize the contrast of the old population contributing to the RGB. Since all the galaxies under study are located relatively far from us, their TRGB position is close to the photometric limit. In

such cases, the RGB luminosity function may not have the clear discontinuity necessary for an application of the maximum likelihood method. In such cases, the TRGBtool program uses a simple age detection algorithm, which can result in larger TRGB uncertainties. Five galaxies from our sample (UGC 3600, UGC 3698, NGC 2337, UGC 3860, UGC 5288) have RGB luminosity functions that are too smooth for the maximum likelihood calculation. The calibration of the absolute value of the TRGB including a small color term has been described by Rizzi et al. (2007). The RGB is redder for older or more metal rich populations but galaxies inevitably have old and metal poor components, resulting in reasonable stability of tip magnitudes in the F814W band. The F814W band is favorable because the TRGB luminosity in this band is minimally dependent on age and metallicity effects. Images, color-magnitude diagrams, photometry tables, TRGB measurements, and distance determinations are made available for the newly observed galaxies at <http://edd.ifa.hawaii.edu> by selecting the catalog CMDs/TRGB (Jacobs et al. 2009).

3. TRGB distances to thirteen galaxies

Images of our target galaxies taken from Sloan Digital Sky Survey (<http://www.sdss.org/>) are shown in Figure 1. Each field has a size of 6 by 6 arcminutes. North is up and East is left. The ACS HST footprints are superimposed on the SDSS frames. Figure 2 is a mosaic of enlarged ACS (F606W) images of the galaxies. The field size is 1 arcminute; North is up and East is left. Color-magnitude diagrams (CMDs) of F814W versus (F606W - F814W) are presented in Figure 3. Table 1 provides a summary of basic parameters for the observed galaxies, taken largely from the Updated Nearby Galaxy Catalog (UNGC; Karachentsev et al. 2013), as well as new TRGB and distance measurements. There is the following information in the table columns: (1) common galaxy name, (2) Principal Galaxies Catalog

number, (3) equatorial coordinates, (4-5) supergalactic coordinates, (6-8) heliocentric, Local Sheet, and Local Supercluster velocities, (6) major diameter measured at the Holmberg 26.5 mag/square arcsec isophote in arcmin, (7) apparent integrated B magnitude, (8) morphological type on the de Vaucouleurs numeric scale, (9) TRGB magnitude, (9) Galactic extinction in the I- band (Schlafly & Finkbeiner, 2011), (10) the linear distance, in Mpc, and 68% probability error.

Two objects of low surface brightness, KK 69 and KK 70, are close physical companions to the spiral NGC 2683 with projected separations of 62 and 89 kpc, respectively. The other targets besides NGC 2683 are dwarf galaxies of morphological types Irr, Im, BCD, and Sm. According to the UNGC, the mean stellar density in a sphere of radius 1 Mpc around each of these galaxies is about 1/30th of the mean global density of stellar matter. All the dwarfs in the vicinity of NGC 2683 manifest signs of sluggish star-formation as seen from their H-alpha emission, as well as from their flux in the far-ultraviolet (Karachentsev & Kaisina 2013). The average value of the specific star-formation rate for the dwarfs is characterized by the quantity

$$\langle \log(sSFR) \rangle = \langle \log(SFR/M^*) \rangle = -10.10 \pm 0.07 \text{ yr}^{-1},$$

coincident with the value of the Hubble parameter $\log(H_0) = -10.14 \text{ yr}^{-1}$. This agreement is suggestive of a smoldering process where a galaxy, not subject to external influences, reproduces its observed stellar mass over the cosmological time $H_0^{-1} = 13.8 \text{ Gyr}$ quasi-continuously with the presently observed star-formation rate.

4. Peculiar velocities in the Leo Spur

It was demonstrated (Tully et al. 2008; hereafter TSK08) that galaxies in a filament to the south of the Local Sheet in supergalactic coordinates are more distant than would be expected from the Hubble relation; ie, the galaxies have peculiar velocities toward us. The explanation offered, based on a sample of almost 1800 distance measurements around the sky within 3000 km/s, was that the structure that we live in, the Local Sheet, has a motion toward this southern filament due to the expansion of the Local Void to the supergalactic north of us.

The filament to the south has been called the Leo Spur (Tully & Fisher 1987). At the time of the TSK08 discussion, only a few galaxies in the Leo Spur had distance measurements with sufficiently small uncertainties to compel the conclusion that the Leo Spur and the Local Sheet are moving toward each other in co-moving coordinates. The situation now is dramatically improved.

Our current knowledge is demonstrated in three sequences of figures. In each sequence there are three panels. The top panel shows a projection normal to SGY–SGZ, identifying the positions of all galaxies in the volume with distance measurements as reported either in the *Cosmicflows-2* compilation (Tully et al. 2013) or in this paper. The other two panels show the same volume with projections normal to SGY–SGX, split at SGZ=−2, so the middle panel displays the Local Sheet on the supergalactic equatorial plane and the lower panel displays the Leo Spur below the equatorial plane. Colors of symbols identify the techniques used to obtain the distances. The virial regions of the Virgo and Leo clusters are located with filled circles and the domain of the infall region around the Virgo Cluster in the spherical approximation (Karachentsev et al. 2014) is located with the dotted circles.

Only galaxies with known distances are plotted because redshifts are not informative due to severe departures from cosmic expansion. Since nearer galaxies are more likely

to have a known distance, the impression of the distribution of galaxies is biased. The representation of the Leo Spur is skeletal. Nonetheless we see the important aspects. The Leo Cluster is situated just outside the nominal edge of the Virgo infall domain. The region between the Leo and Virgo clusters appears to be sparsely populated. In the top panel of Figure 4 we see that the Leo Spur lies in a band that is slightly sloped in SGZ roughly 5 Mpc below the Local Sheet. There is a filament that runs slightly to the background from the modest Leo Cluster to $SGX \sim 10$ Mpc at roughly constant $SGY \sim 11$ Mpc, and represented extremely sparsely here by three galaxies with Cepheid distances, NGC 2841, NGC 3198, and UGC 4284. A second closer, hence better represented, strand runs through the galaxies NGC 2903³ and NGC 2683 to the region of the galaxy NGC 2337. This nearer domain is accessible to TRGB distance measurements with single orbit observations with HST. The Local Sheet and Leo Spur only partially overlap in an SGX–SGY projection, with the Leo Spur running to larger values of SGX. The nest of galaxies around UGC 3974 lies slightly apart from the nearer strand. This group is of particular interest because of its location near the supergalactic south pole where it receives almost the full reflex of our motion away from the Local Void.

The second and third sequences show the same scenes but add peculiar velocity vectors in two reference frames. In that second sequence, Figure 5, the reference frame is the Local Sheet (TSK08) and cosmic expansion is removed assuming $H_0 = 74$ km/s/Mpc. The reference frame is essentially the same as the various versions of the Local Group frame. Reasonable variations of the Hubble Constant have only small effects on the analysis.

The third sequence of Figure 6 is in what TSK08 called the Local Supercluster rest frame. This reference frame nulled our motion with respect to all galaxies with measured

³NGC 2903 does not yet have a good distance measurement; we give it the average distance of 2 neighbors.

distances within 3000 km/s. The transformation from Local Sheet coordinates can be separated into two vectors: a motion of 185 km/s directed toward the Virgo Cluster and a motion of 259 km/s directed almost due south in supergalactic coordinates, away from the Local Void.

The two sequences demonstrating peculiar velocities reveal marked local coherence. In the second sequence, that in a local frame of reference, it is seen that galaxies within 8 Mpc lying within the supergalactic equatorial plane of the Local Sheet have only small peculiar velocities. Nearby galaxies in the Local Sheet are moving together in co-moving coordinates. In this second sequence, essentially every other galaxy, those beyond 8 Mpc or not in the Local Sheet, has a substantial peculiar velocity toward us.

In the third sequence, that in the Local Supercluster reference frame, the pattern of motions is quite different. In this reference frame, the Local Sheet is moving toward +SGY (toward Virgo) and –SGZ (away from the Local Void). Galaxies in the region of the Virgo Cluster have essentially zero velocity in this reference frame. Along the Leo Spur the peculiar velocities in the third sequence are mixed. Motions are slightly positive at the end toward the Leo Cluster and increasingly negative at greater distances from Virgo. The positive velocities toward Virgo can be anticipated as due to the approach to the Virgo infall zone (not modeled here). Negative peculiar velocities at the more distant regions from Virgo could alternatively be due to an underestimate of the motion of the Local Sheet away from the Local Void or to a peculiar motion of the Leo Spur toward positive SGZ because of a push from the Gemini–Leo Void.

The main conclusion of this section is that the Local Sheet motions identified in TSK08 are basically confirmed with, now, a substantial body of distance measurements based on HST observations of the luminosities of tip of the red giant branch sequences. Inspection of the color-magnitude diagrams that are presented will reveal that the tip locations are near

the limit of the methodology with one-orbit observations. However there is no doubt that the targets are more distant than expected from Hubble flow (tips would be brighter, hence more easily determined, if they were closer) and that peculiar velocities in the Leo Spur, are strongly negative in the Local Sheet frame. With the data analyzed in this paper alone it can only be said that the Local Sheet and Leo Spur have motions toward each other in co-moving coordinates. From consideration of data on larger scales it is clear that the Local Sheet departs from the cosmic microwave background frame with a motion away from the Local Void and toward the Leo Spur. Whether downward motion of the Local Sheet is the whole story or Leo Spur has an upward motion, as suggested by residuals from the TSK08 model seen in Figure 6, these possibilities await a new analysis of distance data over a much larger domain.

5. Dwarf Associations

The complementarity of all-sky searches for nearby galaxies (Karachentseva & Karachentsev 1998 and following), accurate radial velocities from HI follow ups (Huchtmeier et al. 2001), and HST TRGB distance measurements for now almost 400 galaxies has led to a detailed picture of the structure of groups in our vicinity. Most galaxies in a volume limited sample are dwarfs. Many dwarfs are found near giant galaxies but it is of considerable interest that dwarfs also gather with other dwarfs. There are very few extremely isolated dwarfs.

Tully et al. (2006) referred to regions crowded with dwarfs as associations and drew attention to seven such entities within 8 Mpc that share the following properties: no high luminosity member, 4 – 6 dwarfs, scales of ~ 300 kpc, and radial velocity dispersions 10 – 40 km/s. Characteristic crossing times are a substantial fraction of the age of the universe so it is unlikely that the systems are in equilibrium, but if they are bound then their masses

are in the range $10^{11} - 10^{12} M_{\odot}$ and mass-to-blue-light values are several hundred to a thousand.

The most distant of the associations identified in the 2006 paper lies in the Leo Spur around the galaxy UGC 3974, labeled in Figs. 4–6. Three tightly linked galaxies and an outrider were called the 14+19 Association⁴, their identification in the Nearby Galaxies Catalog (Tully 1988b). Today, three more dwarf galaxies have been identified in close proximity and with similar velocities. Two of these, AGC 174585 and AGC 174605, have TRGB distances. The velocity dispersion of the 6 is very small, 21 km/s. However the projected separations of the newly discovered companions are of order 700 kpc. A halo with mass $5 \times 10^{11} M_{\odot}$ is expected to have a virial domain of only 170/210 kpc (projected/3D) and an infall domain restricted to 500/610 kpc (Tully 2015). Only two galaxies in the ensemble, UGC 3974 and KK 65, lie in a common collapsed halo and only one more, UGC 4115, teeters on the edge of infall toward those two. UGC 3775 and the two AGC systems are each in separate halos and in expansion from the association unless there is a very large amount of unseen matter.

The new distance information draws attention to an association around NGC 2337, in an entity called 15+12 in the Nearby Galaxies Catalog. There are four galaxies in the region with TRGB distance measures⁵ and two more known with excellent velocity matches. However the situation is similar to that of the 14+19 Association. Only two galaxies, NGC 2337 and UGC 3698, are likely to lie in a common halo and one more, UGC 3817, probably lies within a related infall zone. The velocity dispersion for these three is a minuscule 5 km/s in the line-of-sight. Another pair, UGC 3860 and UGC 3966, probably lie within a

⁴In Tully (1988b) the entity was erroneously linked to the 14 cloud, now called the Local Sheet, because of its low systemic velocity; the Leo Spur is cloud 15 in that reference.

⁵UGC 4426 is a fifth galaxy but it is 2 Mpc from any of the others.

common but distinct infall zone ~ 1.5 Mpc away. UGC 3600 is expanding away from these others unless the dark matter concentration is in an extreme disproportion to the visible matter.

6. Concluding remarks

The Leo Spur is the nearest distinct large scale structure outside of the Local Sheet. Systemic velocities in the Leo Spur are modest but already with the identification of the local velocity anomaly (Faber & Burstein 1988, Tully 1988a) departures in this region from Hubble expansion were noticed. Galaxies in the Leo Spur are more distant than would be supposed from their velocities. In the course of the analysis of the distance compilation *Cosmicflows-1* (TSK08), a model was developed that provided an explanation. A key observational element is the *discontinuity* in peculiar velocities between those in the Local Sheet and those in the Leo Spur. It was inferred that the Local Sheet is descending toward the negative supergalactic pole due to the expansion of the Local Void. The Leo Spur is decoupled from this expansion, hence, the two structures have relative motions toward each other in co-moving coordinates.

While the distance information in TSK08 was limited, the observational situation is considerably improved today with the publication of *Cosmicflows-2* (Tully et al. 2013) and recent imaging with HST that results in the TRGB distance estimates presented here, supplement by contributions by McQuinn et al. (2014). The new material emphatically confirms relevant aspects of the TSK08 model. The accumulated distance information demonstrates the spatial separation and kinematic discontinuity between the Leo Spur and the Local Sheet. The velocity field in the region embracing the Leo Spur, Local Sheet, and Virgo Cluster displays three overriding features in the Local Sheet reference frame: (1) galaxies within the Local Sheet have very small peculiar velocities around

the cosmic expansion, (2) galaxies in and around the Virgo Cluster have large negative peculiar velocities, and (3) galaxies in the Leo Spur have large negative peculiar velocities. According to the TSK08 model, the galaxies of the Local Sheet are responding together to two relatively local influences: an attraction toward the Virgo Cluster causing a motion of 185 km/s and a repulsion away from the Local Void causing a motion of 259 km/s.

The reference frame referred to as ‘local supercluster’ incorporates this simple model. It is seen in transitioning from the scenes of Fig. 5 to the scenes of Fig. 6 that (1) galaxies in the Local Sheet are streaming toward the Virgo Cluster, (2) Virgo is practically at rest, and (3) the flow pattern in the Leo Spur has been largely nulled out. There is a slight trend along the Leo Spur toward positive velocity residuals near the Leo Cluster and negative residuals at the far reaches from Leo. Such a pattern can be explained by the attractive influence of the Virgo Cluster near the Leo Cluster as the Virgo infall zone is approached (Karachentsev et al. 2014) and the repulsive influence of the Gemini-Leo Void that lies below the Leo Spur.

In Tully et al. (2008) it was pointed out that a completely empty void in a topologically flat Λ CDM universe with matter contributing 24% of the critical density expands at 16 km/s/Mpc. This expansion rate was derived in two ways: analytically from the Friedman equation assuming spherical symmetry and from n-body simulations (van de Weygaert & Schaap 2007). If a void is not empty, the expansion is reduced. It follows that the convergence of the Local Sheet and Leo Spur at ~ 260 km/s provides information regarding a combination of the size and emptiness of the voids at their edges. This large motion implies large voids.

It is to be appreciated that the clear identification of peculiar motions away from voids is possible in the present situation because (1) individual peculiar velocities are large compared with uncertainties coming from distance errors and (2) the geometry is such that

we can see the full amplitude of motions in radial velocities. We are afforded insight into the properties of voids due to our proximity to the Local Void that is otherwise not easily available.

The 2008 model deserves to be refined in the light of the new distance information. However, if only peculiar velocities within the restricted domain explored in this paper are considered then only the relative convergence of the Local Sheet, Leo Spur and Virgo Cluster components can be evaluated; but not the relative importance of the external influences. To properly evaluate the relative influences of the downward push of the Local Void versus the upward push of the Gemini-Leo Void, it will be necessary to give attention to distances and the velocity field over a much larger volume, a task for later study.

As the name implies, the Leo Spur is not a major feature. The strand nearest us that is most easily studied peters out into associations of dwarfs. Such regions are of interest because they may be the visible manifestations of halos at masses below $10^{12} M_{\odot}$. Dwarf galaxies that lie apart from major galaxies tend to flock together. However, in the two cases presented in the Leo Spur, the 14+19 and 15+12 associations, only a few of the dwarfs are likely to be bound to each other unless there is a lot more dark matter in their vicinity than supposed.

Acknowledgements: This work is based on observations made with the NASA/ESA Hubble Space Telescope. STScI is operated by the Association of Universities for Research in Astronomy, Inc. under NASA contract NAS 526555. The work in Russia is supported by RFBR grants 13–02–90407 and 13–02–92960. L.N.M. and D.I.M. acknowledge support from RFBR grant 13–02–00780 and Research Program OFN17 of the Division of Physics, Russian Academy of Sciences.

References

- Brinckmann T., Lindholmer M., Hansen S.H., Falco M., arXiv:1411.6650
- Cautun M., van de Weygaert R., Jones B.J.T., Frenk C.S., 2014, MNRAS, 441, 2923
- Dolphin, A. 2000, PASP, 112, 1383
- Elyiv A.A., Karachentsev I.D., Karachentseva V.E., Melnyk, O.V., Makarov D.I., 2013, Astophys. Bulletin, 68, 1
- Faber S.M., Burstein D., 1988, in Large-Scale Motions in the Universe (Princeton: Princeton Univ. Press), 115
- Huchtmeier, W.K., Karachentsev, I.D., Karachentseva, V.E. 2001, A&A, 377, 801
- Jacobs, B.A., Rizzi, L., Tully, R.B. et al. 2009, AJ, 138, 332
- Jacobs, B.A., Tully, R.B., Rizzi, L., et al. 2011, AJ, 141, 106
- Karachentsev, I.D., Kaisina, E.I. 2013, AJ, 146, 46
- Karachentsev I.D., Makarov D.I., Kaisina E.I., 2013, AJ, 145, 101 (UNGC)
- Karachentsev I.D., Makarov D.I., Sharina M.E., et al., 2003, A & A, 398, 479
- Karachentsev, I.D., Tully, R.B., Wu, P.-F., et al. 2014, ApJ, 782, 4
- Karachentseva, V.E., Karachentsev, I.D. 1998, A&AS, 127, 409
- Makarov, D.I, Makarova, L., Rizzi, L. et al. 2006, AJ, 132, 2729
- McQuinn K.B.W., Cannon J.M., Dolphin A.E. et al. 2014, ApJ, 785, 3
- Peebles P.J.E., 1980, The Large-scale structure of the universe, Princeton University Press
- Rizzi L., Tully R.B., Makarov D.I., et al., 2007, ApJ, 661, 813

- Schlaflly, E.F., Finkbeiner, D.P., 2011, ApJ, 737, 103
- Shandarin S., Habib S., Heitmann K., 2012, Physical Review D., 85, 8
- Shandarin S. F., Klypin A. A., 1984, SvA, 28, 491
- Shandarin S. F., Zeldovich Y. B., 1989, Rev. Mod. Phys., 61, 185
- Tully R.B., 2015, AJ, 149, 54
- Tully R.B., Courtois H.M., Dolphin A.E. et al. 2013, AJ, 146, 86
- Tully, R.B., Fisher, J.R. 1987, Nearby Galaxies Atlas (Cambridge Univ. Press)
- Tully R.B., Shaya E.J., Karachentsev I.D., Courtois H.M., Kocevski D.D., Rizzi, L., & Peel, A. 2008, ApJ, 676, 184 (TSK08)
- Tully R.B., Rizzi L., Dolphin A.E., Karachentsev I.D. et al., 2006, AJ, 132, 729
- Tully R.B., 1988a, in Large-Scale Motions in the Universe (Princeton: Princeton Univ. Press), 169
- Tully R.B., 1988b, Nearby Galaxies Catalog (Cambridge Univ. Press)
- Zeldovich, Ya.B., 1970, A& A 5, 84
- van de Weygaert, R., Schaap, W., 2007, in Data Analysis in Cosmology, ed. V. Martinez et al. (Berlin: Springer), arXiv:0708.1441
- van Haarlem, M., van de Weygaert, R., 1993, ApJ, 418, 544

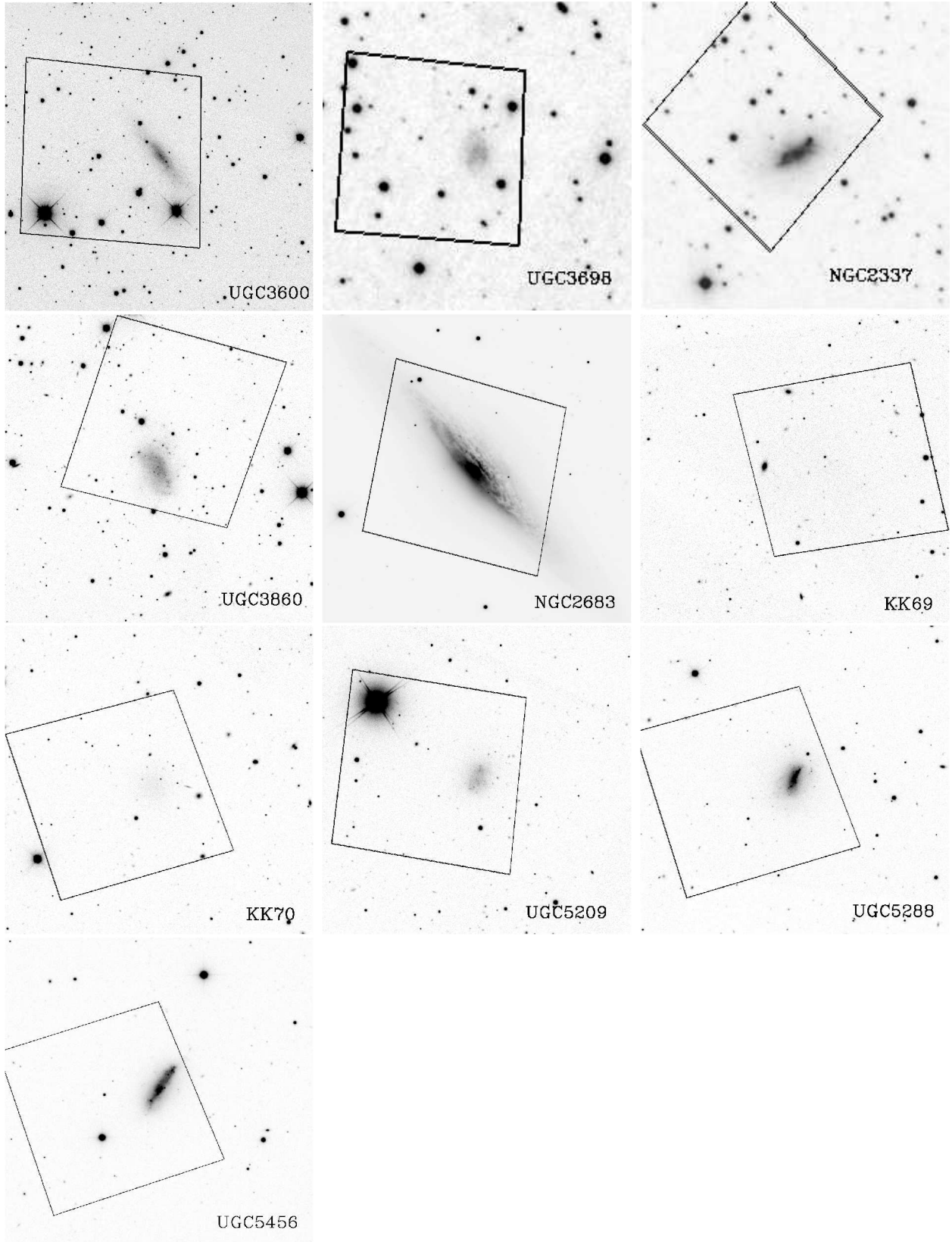


Fig. 1.— Sloan Digital Sky Survey images of target galaxies. Each field has a size of 6 by 6 arcminutes. North is up and East is left. The HST ACS footprints are superimposed.

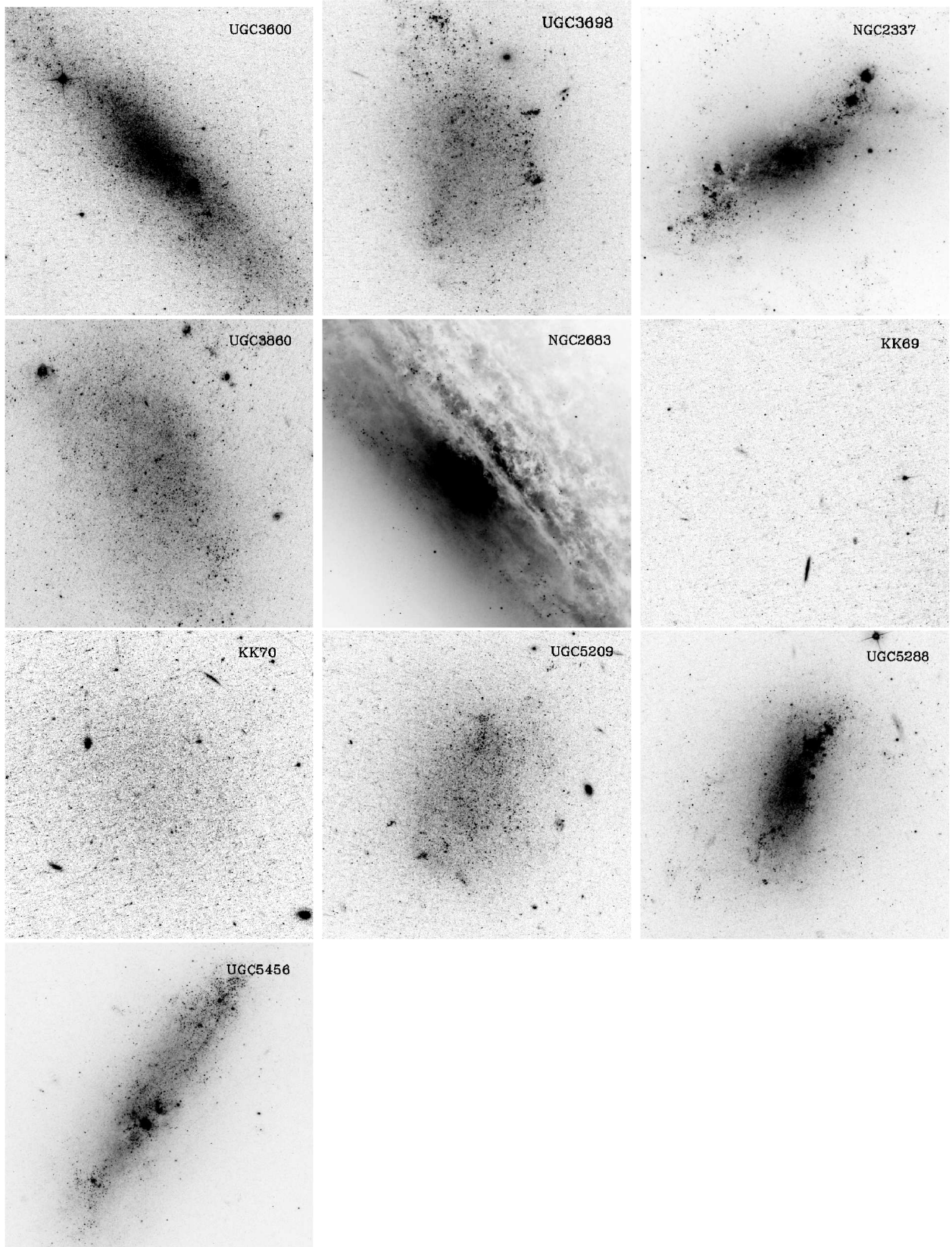


Fig. 2.— Mosaic of enlarged ACS F606W images of the galaxies. Field sizes are 1 arcminute on a side, North is up and East is left.

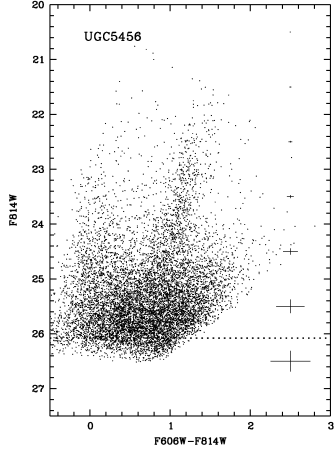
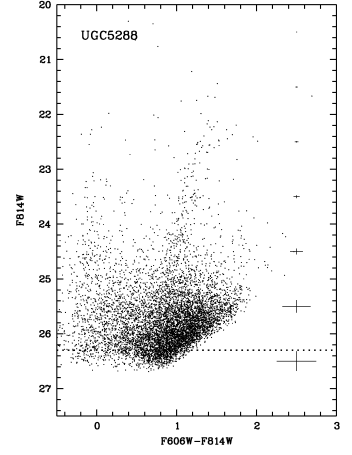
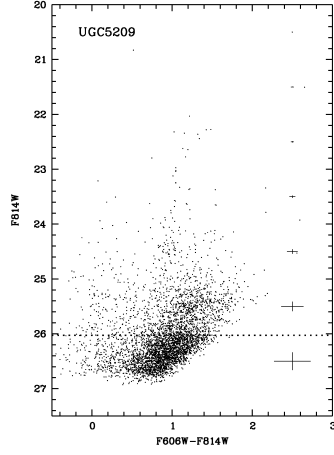
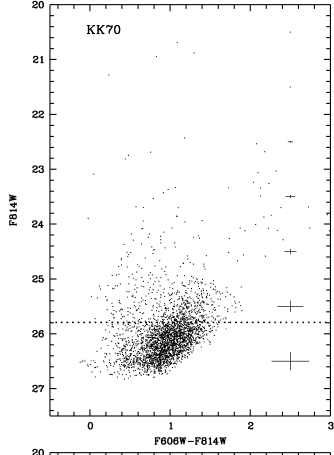
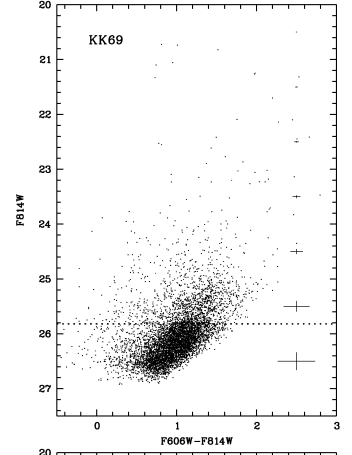
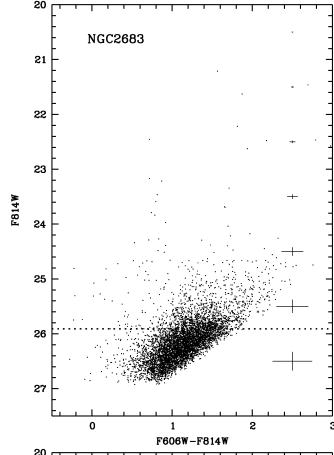
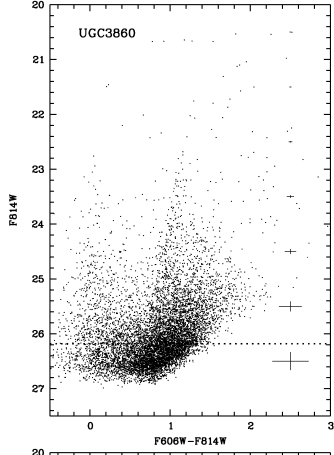
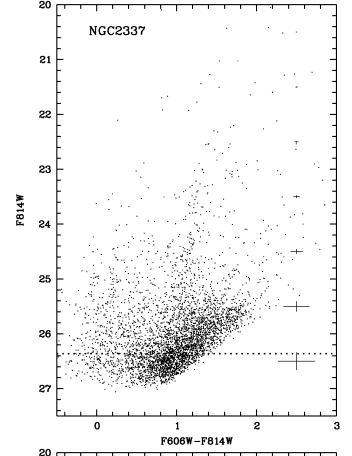
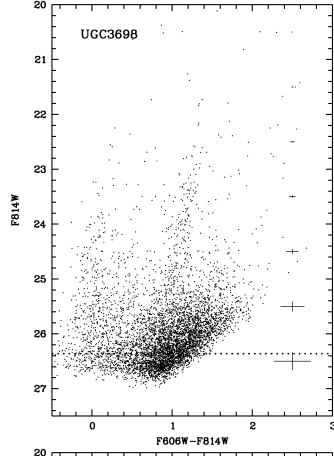
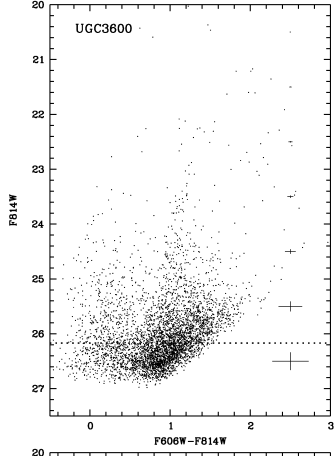


Fig. 3 caption. Color-magnitude diagrams for target galaxies from ACS observations. The dotted horizontal lines mark the magnitudes of the TRGB.

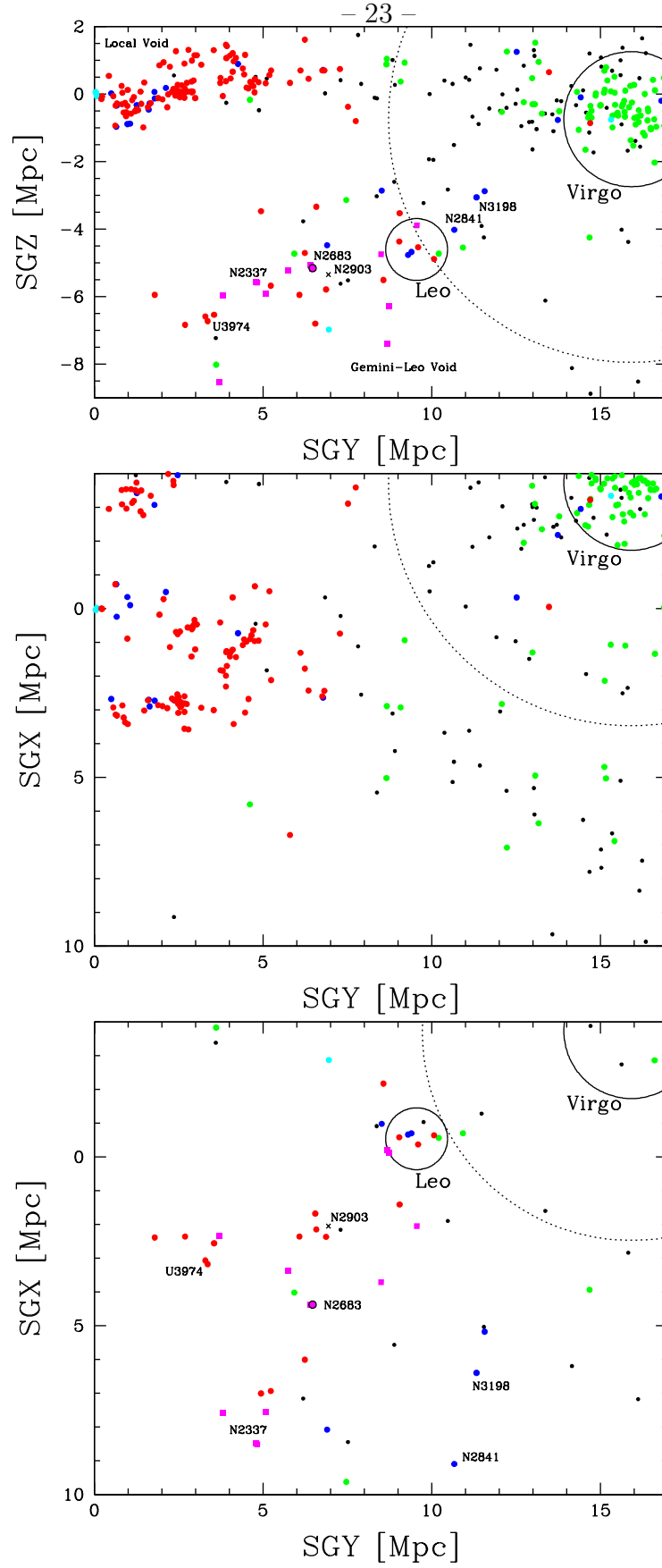


Fig. 4.—

Fig. 4 caption. Projections of the Leo Spur region in supergalactic coordinates. Top: SGY–SGZ view with $-4 < SGX < +10$ Mpc. Mid and bottom: SGX–SGY views split $+2 > SGZ > -2$ and $-2 > SGZ > -9$ Mpc to isolate the Local Sheet in the middle panel and the Leo Spur in the bottom panel. Symbol colors identify sources of distance measurements: blue – cepheid; green – SBF; red – previous TRGB; magenta squares – new TRGB. Important galaxies are identified. Solid circles: Virgo and Leo cluster virial regions. Dotted circles: Virgo Cluster infall region. The Local and Gemini-Leo voids are extensive regions above the Local Sheet and below the Leo Spur, respectively, in SGZ.

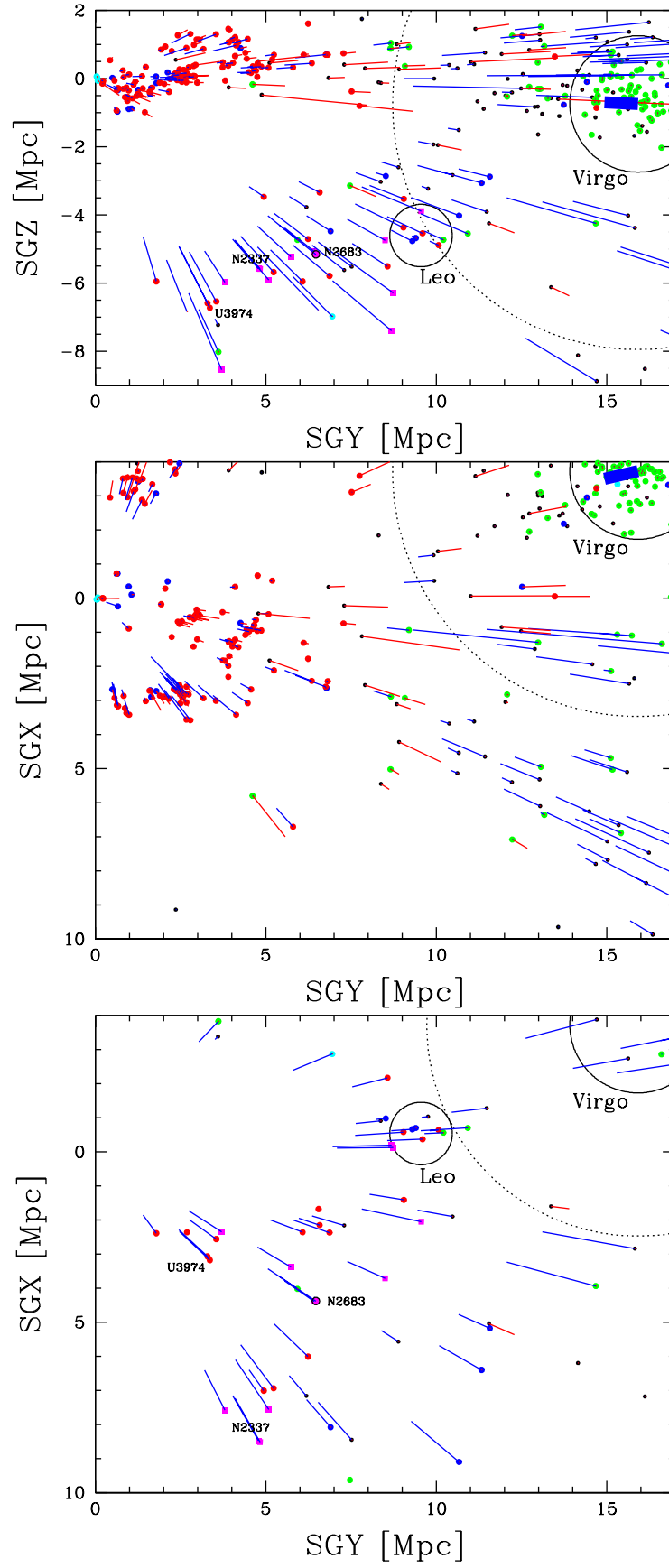


Fig. 5.—

Fig. 5 caption. Same as Fig. 4 with the addition of line-of-sight peculiar velocity vectors in the Local Sheet reference frame, assuming $H_0 = 74$ km/s/Mpc. Negative peculiar velocity vectors are blue and toward us while positive peculiar velocity vectors are red and directed away. The heavy blue vector at the Virgo Cluster is an average for the entire cluster. Scale: vector 1 Mpc in length = 200 km/s.

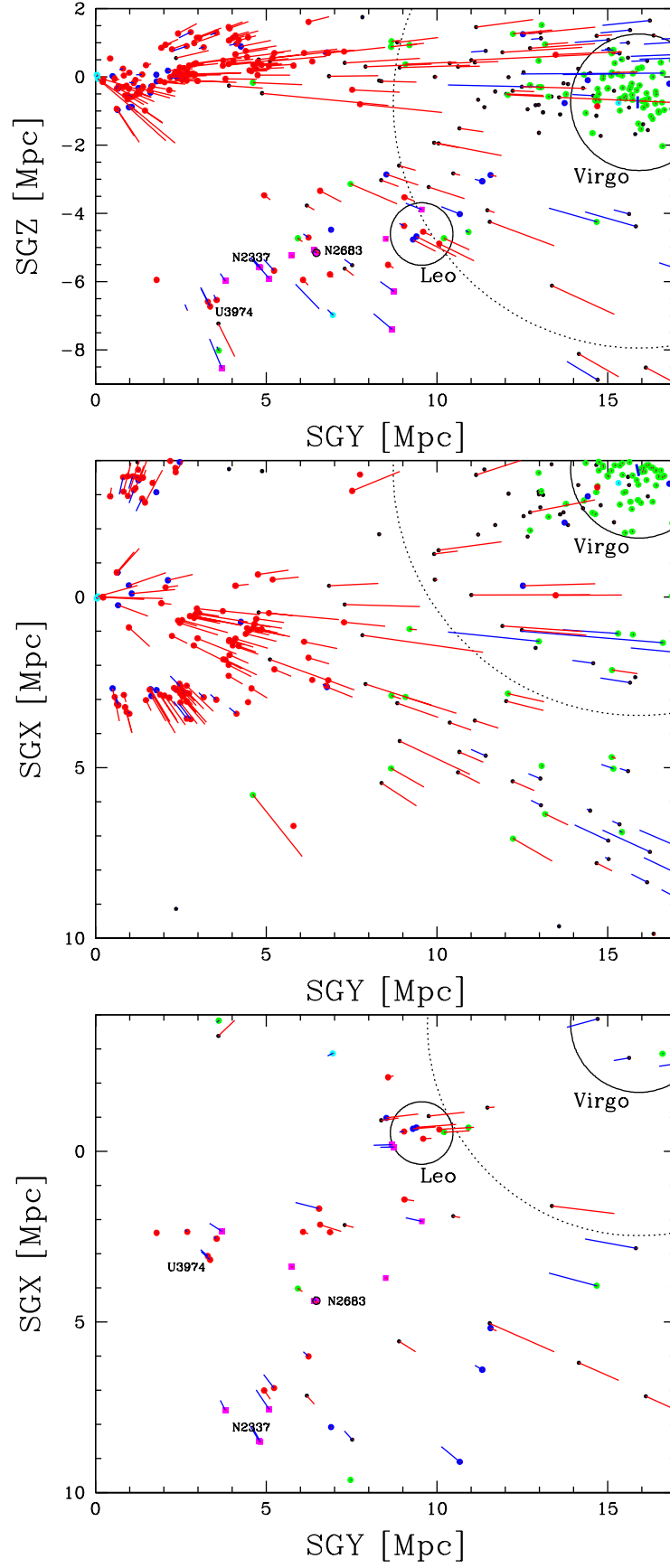


Fig. 6.—

Fig. 6 caption. Same as Fig. 5 except in the Local Supercluster reference frame, assuming $H_0 = 74$ km/s/Mpc. Negative peculiar velocity vectors are blue and toward us while positive peculiar velocity vectors are red and directed away. The averaged Virgo Cluster vector is only slightly negative. Scale: vector 1 Mpc in length = 200 km/s.

Table 1: Galaxies in the Leo Spur recently observed with HST.

Name	PGC	RA (J2000) Dec	SGL	SGB	V_h	V_{LS}	V_{LSC}	a_{Ho}	B_T	T	I_{TRGB}	A_I	D_{TRGB}
UGC3600	19871	065540.0+390542	26.60	-35.20	412	448	693	1.91	16.2	8	26.17	0.17	10.38±1.02
UGC3698	20264	070918.8+442248	29.39	-29.82	422	479	716	1.17	15.4	10	26.36	0.18	11.22±1.11
NGC2337	20298	071013.6+442725	29.58	-29.73	436	493	730	2.75	13.5	9	26.36	0.17	11.28±0.57
UGC3860	21073	072817.2+404613	33.96	-33.00	354	386	641	1.41	15.1	10	26.18	0.11	10.86±1.34
NGC2683	24930	085240.9+332502	55.87	-33.42	411	381	673	13.49	10.3	3	25.91	0.06	9.36±0.28
KK69	166095	085250.7+334752	55.64	-33.09	463	435	726	1.38	17.4	10	25.82	0.06	9.28±0.28
KK70	166096	085522.0+333333	56.32	-32.98	–	–	—	0.50	17.7	-3	25.79	0.06	9.18±0.30
UGC5209	27935	094504.2+321418	66.40	-27.11	538	498	787	0.83	16.1	10	26.03	0.04	10.42±0.35
UGC5288	28378	095117.2+074938	91.28	-40.42	556	390	703	1.45	14.6	9	26.30	0.07	11.41±1.10
UGC5456	29428	100719.6+102143	90.82	-35.73	544	391	699	1.62	13.8	9	26.08	0.06	10.77±1.07
AGC174605	5060076	075021.7+074740	57.66	-62.79	351	206	517	0.34	18.0	10	25.83	0.04	9.60±0.18
AGC182595	4087020	085112.1+275248	59.52	-38.12	396	336	640	0.36	17.2	9	25.61	0.07	8.47±0.14
AGC731457	1824266	103155.8+280134	77.87	-21.68	454	396	675	0.38	16.8	10	26.07	0.04	10.52±0.34